Iran. J. Biotechnol. January 2023;21(1): e 3180 DOI: 10.30498/ijb.2022.310632.3180

Research Article

Evaluation of Apoptosis, Cell Proliferation and Cell Cycle Progression by Inactivation of the NEAT1 Long Noncoding RNA in a Renal Carcinoma Cell Line Using CRISPR/Cas9

Nastaran Haghighi[1], Abbas Doosti[2*], Jafar Kiani[1,3]

[1]Department of Biology, Faculty of Basic Sciences, Shahrekord Branch, Islamic Azad University, Shahrekord, Iran.
[2]Biotechnology Research Center, Shahrekord Branch, Islamic Azad University, Shahrekord, Iran.
[3]Department of Molecular Medicine, Faculty of Advanced Technologies in Medicine, Iran University of Medical Sciences (IUMS), Tehran, Iran.

[*]*Corresponding author*: Abbas Doosti, Biotechnology Research Center, Shahrekord Branch, Islamic Azad University, Shahrekord, Iran, P.O. Box: 166, Shahrekord, Iran. Tel: +98- 3833361048, Fax: +98-3833361001, E-mail: abbasdoosti@iushk.ac.ir

Received: 2021/10/16; **Accepted:** 2022/03/06

Background: Long noncoding RNAs (lncRNAs) play an important role in cellular mechanisms including transcription, translation, and apoptosis. *NEAT1* is one of the essential types of lncRNAs in humans that can bind to active genes and modify their transcription. *NEAT1* upregulation in various forms of cancer such as kidney cancer has been reported. Kidney cancer accounts for approximately 3% of all cancers worldwide and occurs almost twice as often in men as in women.

Objectives: This study has been performed to knockout the *NEAT1* gene using the CRISPR/Cas9 technique in the Renal Cell Carcinoma ACHN cell line and to evaluate its effects on cancer progression and apoptosis.

Material and Methods: Two specific (single guide RNA (sgRNA) sequences for the *NEAT1* gene were designed by CHOPCHOP software. These sequences were then cloned into plasmid pSpcas9, and recombinant vectors PX459-sgRNA1 and PX459-sgRNA2 were generated. *ACHN* cells were transfected using recombinant vectors carrying sgRNA1 and sgRNA2. The expression level of apoptosis-related genes was assessed by real-time PCR. Annexin, MTT and cell scratch tests were performed to evaluate the survival, proliferation, and migration of the knocked out cells, respectively.

Results: The results have shown successful knockout of the *NEAT1* gene in the cells of the treatment group. Expressions of *P53, BAK, BAX* and *FAS* genes in the cells of the treatment group (*NEAT1* knockout) showed significant increases in expression compared to the cells of the control group ($P < 0.01$). Additionally, decreased expression of *BCL2* and *survivin* genes was observed in knockout cells compared to the control group ($p < 0.05$). In addition, in the cells of the treatment group compared to control cells, a significant decrease in cell viability, ability to migrate and cell growth and proliferation was observed.

Conclusion: Inactivation of the *NEAT1* gene in ACHN cell line using CRISPR/Cas9 technology elevated apoptosis and reduced cell survival and proliferation which makes it a novel target for kidney cancer therapeutics.

Keywords. ACHN, CRISPR, LncRNA, NEAT1, Renal cell carcinoma

1. Background

Through over 76,000 new cases were diagnosed yearly, kidney cancer is one of the top ten most common cancers worldwide. Men are more likely to be diagnosed with kidney cancer than women. Anyone can develop kidney cancer, but elderly individuals are more likely to develop kidney cancer (those over 75 years old). Survival varies with each stage of kidney cancer.

Generally, the earlier kidney cancer is diagnosed and treated, the better the outcome. Survival by stage of kidney cancer is reported as 5-year observed survival (1). Renal cell carcinomas (RCCs) are the most common type of malignant kidney tumor. It is found in the main substance of the kidney, where filtering occurs. RCC can appear as a single tumor within a kidney or as two or more tumors within the same kidney (2). Approximately 9 out of 10 kidney cancers are renal cell carcinomas. Although RCC usually grows as a single tumor within a kidney, it is possible to simultaneously have two or more tumors in one kidney or both kidneys (3). RCC is classified into several subtypes based on the appearance of cancer cells in the laboratory. Knowing the subtype of RCC can help your doctor determine whether your cancer is caused by an inherited genetic syndrome (4). Despite numerous successes in RCC therapy, treatment regimens and response rates differ among various molecular subtypes (5). The primary goal of treating kidney masses is used to cure people with cancer and to preserve kidney function as much as possible. Protection of kidney function is significant for patients with only one kidney or another type of kidney disease (6). Long noncoding RNAs (lncRNAs) are RNA transcripts that are longer than 200 nucleotides but are not translated into proteins. In recent years, lncRNAs have been discovered to be significant players in various biological functions and gene expression regulation (7). Changes in the expression of certain lncRNAs have been linked to various forms of cancer (8). Many lncRNAs, including HOTAIR (9), MRCCAT1 (9), UCA1 (10), ATB (11), H19 (12), and –FTX (13), have been identified in RCC tumorigenesis and proposed to be important biomarkers for RCC, according to recent studies. Nuclear paraspeckle assembly transcript 1 (*NEAT1*) is a long noncoding RNA that is transcribed from the familial tumor syndrome multiple endocrine neoplasia (MEN) type 1 loci on chromosome 11q13.1 and encodes two transcriptional variants, *NEAT1*-1 (3756 bp) and *NEAT1*-2 (3756 bp - 22,743 bp) (14). Since mice lacking *NEAT1* developed normally, it appears that *NEAT1* is not needed for normal embryonic development or adult life. However, genetic ablation of *NEAT1* resulted in abnormal mammary gland morphogenesis and lactation defects in another case (15). It should be investigated further if the loss of *NEAT1* is consistent with normal cell viability and growth. Since *NEAT1* is responsible for tumor initiation and progression and its recurrent dysregulation in cancers correlates with clinical features such as metastasis, recurrence rate, and patient survival (16), *NEAT1* exhibits typical characteristics of cancer drivers. Because of lncRNA-mediated networks' role in cancer imitation and progression, lncRNAs are studied to develop new therapeutics. Multiple strategies can be used to target lncRNAs (17, 18, 19): (i) lncRNAs can be knocked out using the CRISPR/Cas-9 system; (ii) antisense oligonucleotides (ASOs) and lncRNA-specific siRNAs can be used to knockout lncRNA transcripts. (iii) Small synthetic molecules/peptides/aptamers can be engineered to inhibit and antagonize lncRNA binding to their binding partners (such as protein, DNA, RNA, or other interacting complexes), and (iv) methods to target lncRNAs can be used in conjunction with other treatments, including chemotherapy and radiotherapy, to improve their efficacy (17, 18, 19). Unfortunately, only approximately one in every three patients responds to the treatment, making it critical to find alternative therapies such as CRISPR/Cas9, which is still relatively unknown (20). Initially discovered as a part of the adaptive immune system of bacteria and archaea, the clustered regularly interspaced short palindromic repeats (CRISPR) system was developed into a state-of-the-art technique for editing the human genome. Human cancer cell lines are used to test applications of the CRISPR / Cas9 system in cancer treatment, including cancer modeling and elimination studies (21). CRISPR/Cas9 editing technology is a powerful editing tool. This method uses RNA-guided Cas nucleases to edit the DNA of particular genes. The CRISPRCas9 system has a higher gene knockout yield, and the Cas9 system is easier to build and use. It has been applied to various organisms as the most commonly used gene-editing technology (22). Dysregulation of lncRNAs can promote tumorigenesis and progression of kidney cancer, particularly in renal cell carcinoma, since they regulate major pathways in cell development, proliferation, differentiation, apoptosis, and survival (RCC) (23).

2. Objectives

The aim of this work was to knockout the *NEAT1,* in the renal cell carcinoma ACHN cell line and to study its effects on the expression of some cancer-related genes. In this analysis, we have used a mutant Cas9 nickase (Cas9n) that induces single-strand breaks to

reduce the risk of off-target cleavage and thus improve genome editing specificity. The *NEAT1* knockout ACHN cell line was created using CRISPR/Cas9 gene editing technology, and the effects of *NEAT1* knockout on RCC cancer cell proliferation and migration were investigated *in vitro*. This research may help determine the role and feature of *NEAT1* in RCC.

3. Materials and Methods

3.1. Chemicals and Ethics

RPMI-1640 and FBS were obtained from Gibco (Gibco, NY, USA); Favor Prep™ Plasmid Extraction Mini Kit (FAVORGEN® recommendations, National Biotechnology Park, Taiwan); Lipofectamine™ 2000 (Thermo Fisher Scientific, USA) and puromycin, streptomycin, and penicillin (Sigma–Aldrich, USA); T7 endonuclease 1 (New England Biolabs); TRIzol reagent was obtained from Invitrogen (Invitrogen, Carlsbad, CA, USA); DNase I (Invitrogen, Carlsbad, CA, USA); cDNA synthesize Kit (Biotechrabbit, Berlin, Germany); QuantiTect SYBR Green Master Mix (Qiagen Inc, Germany); cell proliferation MTT Kit I (Roche, Switzerland); Cell Counting Kit-8 (CCK8); Annexin-V-FITC. Propidium iodide eBioscience™ (Invitrogen™, United Kingdom); and Canidium Basic Biosciences).; all the solvents used for extraction were purchased from Caledon and Scharlau (Caledon and Scharlau, Spain). This study was performed with the approval of the Ethics and Research Committees of the Islamic Azad University, Shahrekord, Iran.

3.2. In silico Assay for sgRNA Designing and Vector Construction

The Homo sapiens *NEAT1* gene sequence was found in the GenBank sequence collection of the National Center for Biotechnology Information (National Biosciences, Inc., Plymouth, MN). The *NEAT1* gene and its promoter are 22743 bp in length. Two sgRNAs for locations 16391 to 1410 and 16669 to 16691 of the *NEAT1* gene were designed using the CHOPCHOP website (https://chopchop.cbu.uib.no). The custom sgRNA oligonucleotide AAGACCGATG TTAGTGGCTATG was the sequence of sgRNA1, and AAGACCAGGCTCAGCACAGAC was the sequence of sgRNA2. The pSpcas9 (BB) 2A- Puro V2.0 vector (Addgene), also known as the pSpcas9 vector, was used as the backbone vector in this study. The two sgRNA1 and sgRNA2 were inserted into pSpcas9 vector so that each sgRNA and the cas9 enzyme can be simultaneously expressed when transfected. A pSpcas9-GFP plasmid (carrying the GFP gene) was employed as a control. The recombinant plasmids pSpcas9-sgRNA1 and pSpcas9-sgRNA2 were confirmed using PCR. sgRNA transcription is commonly driven by the human U6 (hU6) promoter. Colony-PCR was performed using the forward primer for the hU6 vector promoter and the reverse primers for sgRNA1 and sgRNA2, as described in **Table 1.** Gene Runner software was used to design the oligonucleotide primers (version 6.5.52).

3.3. In vitro Vector Amplification

The *E. coli* bacteria TOP10F strain was used to transform and amplify the recombinant plasmid. Ampicillin and puromycin are the bacterial and eukaryotic selection markers for the pSpcas9 vector. Then, recombinant vectors were isolated from bacteria using the Favor Prep™ Plasmid Extraction Mini Kit. The purity of the extracted vectors was determined using a NanoDrop spectrophotometer (Thermo Scientific™ NanoDrop 2000, Wilmington, DE, USA) and an absorbance ratio of 260 nm relative to 280 nm was measured for quality check, as described by Sambrook and Russell 2001 (24).

3.4. Cell Culture and Plasmid Transfection

In this study, a human RCC cell line (ACHN) (NCBI_ Iran; C206) was purchased from Pasture Institute (Tehran, Iran), immediately frozen in liquid nitrogen, and stored at -80 °C until further analysis. ACHN cells were maintained in RPMI-1640 (Gibco, NY, USA) medium. Cell medium was supplemented with 10% v.v fetal bovine serum (Gibco, NY, USA), 100 $\mu g.mL^{-1}$ penicillin and 0.1 $\mu g.mL^{-1}$ streptomycins in a humidified atmosphere containing 5% CO_2 at 37 °C. ACHN cells were transferred to a 6-well plate for transfection after reaching 75% confluence and incubated for 24 hours. The pSpcas9-sgRNA1 and pSpcas9-sgRNA2 were then co-transfected into ACHN cells using Lipofectamine 2000 (Thermo Fisher Scientific, USA) according to the manufacturer's standard instructions. The cells were transfected with the pSpcas9-GFP vector in the control group (pSpcas9-group). A cell culture medium containing 2 $\mu g.mL^{-1}$ puromycin was replaced 24 hours after transfection to screen transfected cells (puromycin

Table 1. The details of oligonucleotide primers that were used for PCR and real-time PCR.

Target	Primers Name	Sequences 5'→3'	Annealing Temperature (°C)	Product length (bp)
NEAT1	*NEAT1* –F	CTTTCATCTGCTTGTTCGTGCTC	62	Non digest:1001 Digest:590
	NEAT1 –R1	ACCTCGAACTCCTAGCCTCCTC		
	NEAT1 –R2	CTTGTGCACTCTTGGTGAGAAC		
NEAT1 -RT-qPCR	q-*NEAT1* - F	AACATTCCATTCCCTCCAGC	62	134
	q-*NEAT1* -R	GTGCTCAGAGAAATAAGCCAGTC		
pSpcas9-sgRNA1	hU6-P- *NEAT1* -sg1	GAGGGCCTATTTCCCATGATT AAGACCGATGTTAGTGGCTATG	62	276
pSpcas9-sgRNA2	hU6-P- *NEAT1* -sg2	GAGGGCCTATTTCCCATGATT AAGACCAGGCTCAGCACAGAC	62	276
P53	*P53*-F	TGCGTGTGGAGTATTTGGATGAC	64	170
	P53-R	CAGTGTGATGATGGTGAGGATGG		
BCL-2	*BCL2*-F	GACGACTTCTCCCGCCGCTAC	65	245
	BCL2-R	CGGTTCAGGTACTCAGTCATCACCAC		
FAS	*FAS*-F	CAATTCTGCCATAAGCCCTGTC	64	163
	FAS-R	GTCCTTCATCACACAATCTACATCTTC		
BAX	*BAX* -F	AGGTCTTTTTCCGAGTGGCAGC	65	243
	BAX -R	GCGTCCCAAAGTAGGAGAGGAG		
BAK	*BAK*-F	CGTTTTTTACCGCCATCAGCAG	66	154
	BAK-R	ATAGCGTCGGTTGATGTCGTCC		
SURVIVIN	*SURVIVIN*-F	AGAACTGGCCCTTGGAGG	64	170
	SURVIVIN-R	CTTTTTATGTTCCTCTATGGGGTC		

NEAT1: Nuclear paraspeckle assembly transcript 1, *pSpcas9:* pSpcas9 (BB) 2A- Puro V2.0 vector, *Bcl2:* B-cell lymphoma 2, *BAX:* Bcl-2-associated X protein, *BAK:* BCL2 Antagonist/Killer 1 , *P53:* Tumor protein P53, *Fas:* Cell Surface Death Receptor

resistant). Three types of cells were investigated in this study. One group consisted of cells that had not been transfected (blank control group). The cells transfected with the pSpcas9-sgRNA1 and pSpcas9-sgRNA2 plasmids (pSpcas9-sgRNA1/2 group) and the pSpcas9-GFP plasmid (pSpcas9-GFP group) were the other two groups (pSpcas9-group).

Imaging: A Cytation 5 Cell Imaging Multimode Reader (BioTek Instruments, Winooski, VT) with a GFP light cube and a 2x objective was used to photograph GFP-transfected cells. The imager employs a mixture of LED light sources, bandpass filters, and dichroic mirrors to deliver proper wavelength light. The GFP light cube uses a 469per35 excitation filter and a 525per39 emission filter. Object analysis was performed to calculate the number of GFP-positive cells after picture preprocessing to remove background fluorescence from acquired digital pictures. Individual cells were recognized by their fluorescence using an objective analysis of the GFP channel with a threshold of 5000 and a minimum and maximum size selection of 15 μm and 100 μm, respectively.

3.5. Generation of Cell Lines for CRISPR Screening (Isolation of NEAT1 ¯/NEAT1 ¯ Genotypes)

The cell line of the recombinant *NEAT1¯/NEAT1¯* genotypes was isolated from other genotypes using the serial dilution approach. This dilution was performed according to GENECOPOEIA›s recommendations for CRISPR Genome Editing in Cell Lines (25). Briefly, the 96-well plate was filled with 100 µL of fresh RPMI 1640 with 10% FBS. Then, in the first well of the 96-well plate, 200 µL of cell suspension (2×10^4 cells.mL^{-1}) was introduced. The cells in the first were transfected well with sgRNA vectors and grown for 24 hours in the presence of puromycin. Then, 100 µL of the contents of the first well was added to the second well of column one. In the remaining column, one well was diluted in the same way at a 2:1 ratio (i.e., 1:1). One hundred microliters of the second well went into the third well, the third well into the fourth wall, and so on). Next, 100 µL of the contents of column 1 wells were transferred to column 2 wells, and the process was repeated for all columns (i.e., 100 l from all wells of column 2 to column 3), and the plating was incubated in CO_2 for 72 hours. The cellular genomic DNA was extracted and amplified with *NEAT1*-specific primers, given in **Table 1,** in four wells of the plate randomly. Cells with a mutation in both alleles (*NEAT1¯/NEAT1¯*) were identified and proliferated to continue the experiment.

3.6. Gene Knockout Confirmation

3.6.1. PCR Amplification

PCR was used to verify sgRNA performance to knockout the *NEAT1* gene. Genomic DNA was extracted from the pSpcas9-sgRNA1, 2 group, blank group, and pSpcas9-group cell lines using the Favor-Prep™ GEL Purification and DNA extraction kit (FAVORGEN Biotech Corp-Taiwan) and PCR amplification. The sequences of oligonucleotide primers for PCR were aligned with GenBank data using NCBI's Basic Local Alignment Search Tool (BLAST). Three primers were designed. The junction of primer F was observed before the target site, primer R2 at the target site, and primer R1 after the target site. If sgRNA binds and cleaves correctly to the target genome, the distance between sgRNA 1 and sgRNA 2 with a length of 8363 nucleotides will be removed. Therefore, a 590 bp fragment will be observed in cells degraded correctly by reacting primers F and R1. In control cells that do not own any sgRNA, the PCR band should be 1001 bp by reacting primers F and R2. If both bands are observed in a PCR product, one allele has been transfected, and the other allele remains intact. PCR amplification of the *NEAT1* gene was carried out in a 25 µL volume of a solution containing 1 µL dNTP mixture with 0.2 µM concentration, 2 µL $MgCl_2$ (2 mM), 2 µL 1X PCR buffer, 1 unit (0.2 µL) Taq DNA polymerase (QIAGEN, Germany), 1 µL (1 µM) forward and reverse primers and 1 µL (50 ng) of DNA with *NEAT1*-specific primers. Then, target genes were amplified using a Biometra thermal cycler (Analytik Jena Co., Germany). The thermal cycler was programmed with the following settings: initial denaturation at 95 °C for 5 minutes, 30 cycles of denaturation at 94 °C for one-minute, annealing temperature at 62 °C for 30 seconds, elongation temperature at 72 °C for 50 seconds, and finally 72 °C for 10 minutes. All samples were electrophoresed on a 1% agarose gel and stained with ethidium bromide. The amplification band of the pSpcas9-sgRNA1/2 group was then compared to that of the pSpcas9 group and the blank group.

3.6.2. RT–PCR and Sequencing

Total RNA was extracted using TRIzol (Invitrogen, Carlsbad, CA) according to the manufacturer's protocol. We used 0.5 µg RNA to synthesize cDNA using the Transcript RT kit (Tiangen Biotech, Beijing, China) with random primers for RT–PCR. Finally, the cDNA obtained was employed in PCR experiments. Based on the primers used, the PCR annealing temperature was 62 °C. To confirm the deletion of the NEAT1 gene, PCR-amplified bands after clean-up were sequenced by the Sanger protocol (Macrogen Inc., South Korea).

3.6.3. Detection of Mismatched Duplexes by T7 Endonuclease Assay

A mismatch-sensitive T7 endonuclease 1 test (New England Biolabs) was used to confirm that DNA cleavage and targeted sequence disruption occurred at the specified spot. DNA was extracted from the pSpcas9-sgRNA1/2 group, pSpcas9-group, and blank group cells using the Favor Prep™ GEL Purification and DNA extraction kit (FAVORGEN Biotech Corp-Taiwan, according to the manufacturer's instructions). In three separate microtubes, 10 µL (200 ng) of each

DNA sample was combined with 2 µL of 10X NE-Buffer 2 buffer and 19 µL of nuclease-free water. At 95 °C for 10 minutes, the samples were heated. Then, it was allowed to cool at room temperature gradually. Nineteen microliters of each sample were combined with 1 µL of T7 endonuclease I (5units.µL^{-1}) and incubated at 37 °C for 15 minutes before being examined on an agarose gel. Band intensities were measured using Tanon-electrophoretic software (Tanon Science & Technology Co., Ltd., Shanghai, China), and the targeted disruption was seen as described by Zhen Shuai (26).

3.7. Expression of Apoptosis-Related Genes by Quantitative Real-Time PCR

The expression of the proapoptotic genes *FAS*, *BAK*, *BAX*, and *P53*, as well as the antiapoptotic genes *BCL2* and *SURVIVIN*, was assessed using a quantitative real-time PCR technique with SYBR green detection. Quantitative real-time PCR was carried out utilizing specific primers (**Table 1**) and an SYBR® Premix Ex Taq™ II kit (TaKaRa, Japan) based on the manufacturer's instructions. A Rotor gene 6000 Corbett system was employed for amplification. Thermal cycling conditions were set as follows: an initial activation step for 5 min at 95 °C, followed by 40 cycles of 95 °C for 15 s and 60 °C for 1 min. Standard curves were created using data from serially diluted samples to confirm the reaction efficiencies of each primer set. Each primer set was also subjected to melt curve analysis. PCR products were electrophoresed on a 1% agarose gel to verify the product size. Relative gene expression levels were quantified by normalizing the GAPDH level. Experiments were conducted in duplicates.

3.8. Cell Viability and Proliferation Assay

(A) CCK-8 assay: The proliferation ability of the pSpcas9-sgRNA1/2 group, pSpcas9 group, and blank group of ACHN RCC cells was assessed using the Cell Counting Kit-8 (CCK-8) assay. ACHN RCC cells were plated at a density of 5× 10^3 cells per well in 96-well plates. After varying incubation times (24 h, 48 h, 72 h, 96 h, and 120 h), 10 µL CCK-8 reagent was added to each well and incubated for another 4 h. Finally, the ability of cells proliferation was assessed using an enzyme-labeled analyzer to measure absorbance at 450 nm.

(B) MTT assay: The cell viability of the pSpcas9-sgRNA1/2 group, blank group, and pSpcas9 group was validated using the cell viability Kit I (MTT) [3-(4,5-dimethylthiazol-2-yl)-2,5-diphenyltetrazolium bromide] (Roche, Switzerland) colorimetric test. In a 96-wellplate, 5 × 10^3 cells/well were cultured at 37 °C in a 5% CO_2 incubator. Cell viability was measured over three days (24 hours, 48 hours, and 72 hours). Each well was filled with 100 µL of serum-free media and 5µg.mL^{-1} Sigma MTT, which was incubated for 4 hours at 37 °C in a CO_2 incubator. The medium was gradually eliminated, and DMSO was introduced. The optical density ratio at 570 nm to the background at 690 nm was measured with a State Fax-2100 ELISA plate reader to detect MTT metabolism and generate blue formazan (Awareness Technology, Palm City, FL).

3.9. Cell Cycle Analysis

Absolute ethanol was used to fix the pSpcas9-sgRNA 1/2 group, blank group, and pSpcas9-group of ACHN cells for 24 hours. The cells were washed twice in PBS before being stained for 15 minutes with BD Bioscience Pharmingen's PI/RNase staining buffer. FACS flow cytometry was used to determine the DNA content of the cell population. FlowJo V10 software was used to evaluate the cell cycle data (Tree Star, Ashland, OR).

3.10. Apoptosis Detection

ACHN cells from the pSpcas9-sgRNA1/2 group, blank group, and pSpcas9 group were washed twice in PBS and then incubated for 15 minutes with FITC-Annexin V (Invitrogen TM, United Kingdom) and PI mixture (BioBasic, Canada). A CyFlow ML flow cytometer was used to examine apoptosis (PARTEC, GERMANY). Multi-Cycle AV software was used to examine apoptosis data *(Phoenix Flow Systems,* Biotechnology Company in San Diego, California).

3.11. Colony Count and Migration Detection

Colony formation assays were conducted to investigate the effects of NEAT1 knockout on ACHN cells proliferation. Eight hundred ACHN cells were seeded onto 6-well plates and incubated for two weeks in complete media. After removing the media, the cells were then fixed with 4% paraformaldehyde and stained with 0.1% crystal violet. Finally, the number of colonies in each well was estimated. In the upper chamber of the Trans well, 10^5 pSpcas9-sgRNA1/2

groups, blank group, and pSpcas9-group ACHN cells were introduced to 600 µL of serum-free media and grown. 600 µL of medium was introduced in the Trans well's lower chamber. The non-invasive cells in the upper chamber were gently removed using a cotton swab after incubating the Trans well at 37 °C for 24 hours.

3.12. Statistical Analysis

All of the trials were carried out three times. The mean difference between groups was estimated using independent T-test or analysis of variance (ANOVA) statistical techniques in the Statistical Package for Social Sciences (SPSS, Inc., Chicago, IL, USA) version 20. GraphPad Prism version 7 for Windows (GraphPad Software, USA) was used to create the graphs. All P values less than 0.05, were considered statistically significant.

4. Results

4.1. In-Silico sgRNA Design

Vector designing strategy including the cleavage site, deleted fragment length, primer binding site, and sgRNA binding are displayed in **Figure 1A**. According to the findings, sgRNAs attach to the *NEAT1* gene segment using the appropriate primers, eliminating the 8363-bp segment. After sgRNA vector construction and bacterial transformation, colonies were selected and checked for the presence and/or absence of sgRNA inserts. PCR and gel results of sgRNA insertion into pSpcas9 vector (pSpcas9-sgRNA1 and pSpcas9-sgRNA 2 vectors) are shown (**Fig. 1B**). 276 bp bands in pSpcas9 vectors show the presence of sgRNA1 and sgRNA2. The 276 bp bands confirmed the presence of sgRNA1 and 2 in vector pSpcas9 in **Figure 1B,** lane 2 and lane 3.

4.2. In Vitro Knockout of the NEAT1 Gene

GFP-containing plasmid devoid of sgRNAs was used to transfect the ACHN cell line to create pSpcas9 (control cell line), which was examined by fluorescence microscopy after 24 hours (**Fig. 1C**). A linear rise in fluorescence when the fraction of GFP-transfected cells was increased to 50k cells/well, was shown (**Fig. 1D**). This finding is comparable to image-based cell counting of GFP-transfected cells. These results show that increasing the fraction of cells constitutively expressing GFP (seeded into wells) results in a 76.8% increase in mean green fluorescence.

Co-transfection of cells using sgRNA vectors can take numerous forms. In the first scenario, a cell group received the vectors pSpcas9-sgRNA1 and pSpcas9-sgRNA2, and both sgRNAs operate on both chromosomal alleles of the *NEAT1* gene, causing cas9 to cleave both alleles. The PCR result in this situation would be a 590 bp fragment, indicating $NEAT1^{-}$/$NEAT1^{-}$ mutation has occurred. However, in other cases, sgRNAs and cas9 may only act on one allele, resulting in the *NEAT1*+/$NEAT1^{-}$mutation, with the PCR output consisting of two 590 and 1001 bp bands.

Among all these options, this study aimed to see how to complete ablation of the *NEAT1* gene (i.e., $NEAT1^{-}$/$NEAT1^{-}$ mutation) affected apoptosis-related genes. As a result, the recombinant cells were screened, and only colonies containing recombinant $NEAT1^{-}$/$NEAT1^{-}$ cells were selected. A 590 bp band indicated that both the *NEAT1* alleles were mutated, and the mutated cells carried the genotype of $NEAT1^{-}$/$NEAT1^{-}$ (**Fig. 2**).

The 590 bp segment should be preserved due to the function of the pSpcas9-sgRNA1 and pSpcas9-sgRNA 2 vectors in cell lines. As a result, the PCR process yielded a 590-bp fragment for the target groups (pSpcas9-*NEAT1*-sgRNA1/2) and a 1001 bp fragment for the control groups (pSpcas9 and Blank) (**Fig. 2A**). The presence of a 590 bp band in the target groups' PCR results demonstrated that sgRNA function was accurate. The T7 endonuclease 1 enzyme was utilized to determine whether the CRISPR sgRNAs solely target the *NEAT1* gene. The 590-bp fragment was extracted from agarose gel electrophoresis and broken out into 179- and 411-bp fragments using the T7 endonuclease 1 enzyme. Mismatch fragments that indicate the right function of sgRNAs are shown (**Fig. 2B)**.

4.3. RT–PCR and Sequencing

Compared to the control group, the DNA sequencing results of the target locations by CRISPR/Cas9-*NEAT1* showed deletion and mutation of the protospacer adjacent motif (PAM) gene fragment. The NHEJ and genomic editing confirm the generation of double-stranded DNA cleavages at specific target DNA sites, resulting in certain mutation patterns (**Fig. 2C)**.

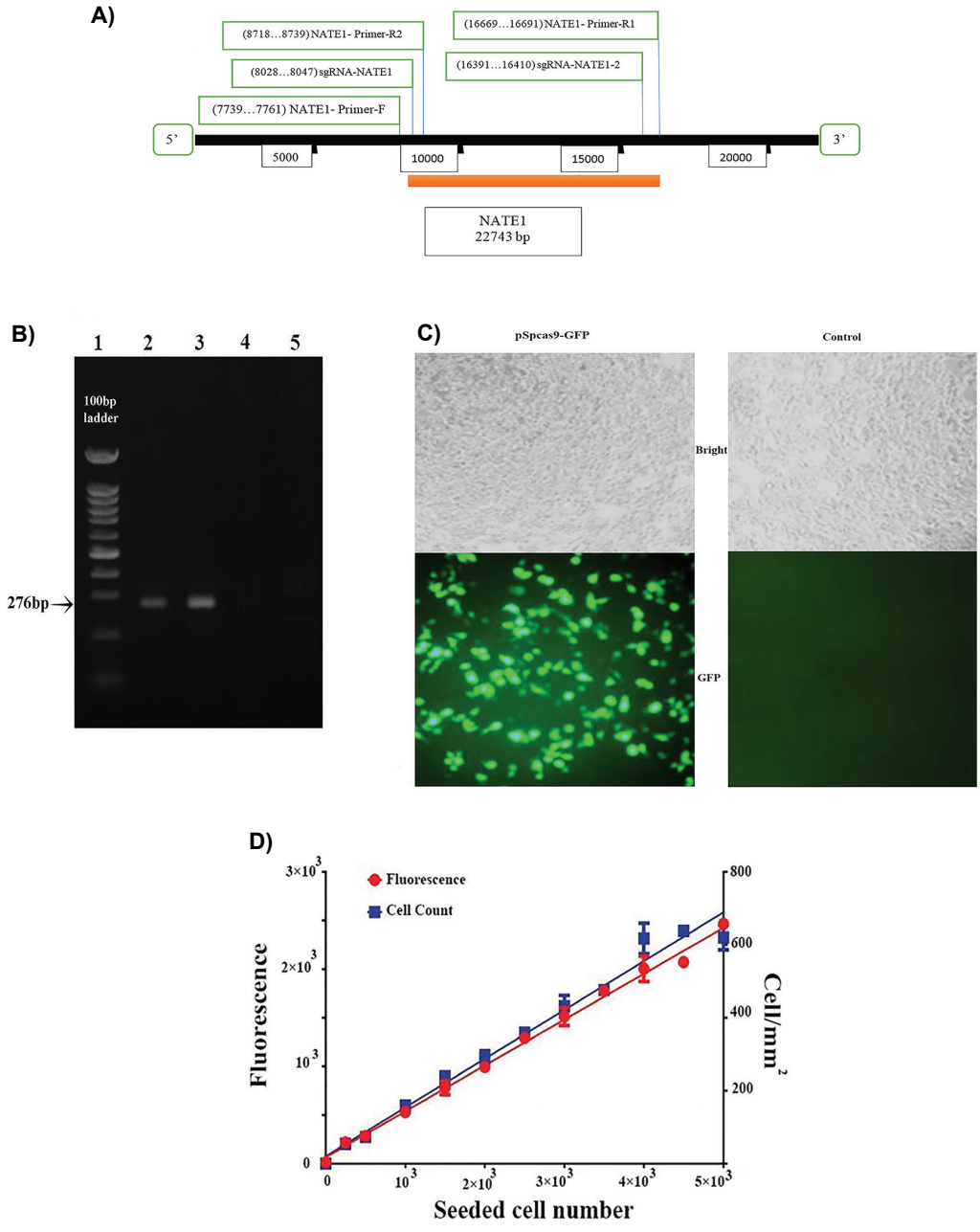

Figure 1. System design and characterization. A) primer binding site, sgRNA binding and cleavage site. **B)** The presence of 276 bp bands in the plasmid vector pSpcas9 verified the existence of sgRNA1 and sgRNA2. Lane 1; 100 bp ladder, lane 2; pSpcas9 -sgRNA1, lane 3; pSpcas9 -sgRNA2, lane 4; pSpcas9 vector, lane 5, Negative control (no DNA). **C)** GFP visibility was used to assess pSpcas9 transfection efficiency. **D)** pSpcas9-GFP ACHN cells were titrated from 0 to 50k cells/well using green fluorescence and image-based cell counts. *pSpcas9: pSpcas9 (BB) 2A- Puro V2.0 vector, GFP: green fluorescent protein.*

RT–PCR was used to examine the relative expression of *NEAT1* in the three groups of RCC cells. The CRISPR/cas9 system in the pSpcas9-sgRNA1/2 group caused *NEAT1* to be degraded, resulting in *NEAT1* being inactive and expression of *NEAT1* approximately being 0. However, *NEAT1* expression was observed in 2 groups: negative control (blank) and positive control (pSpcas9) (**Fig. 2D)**.

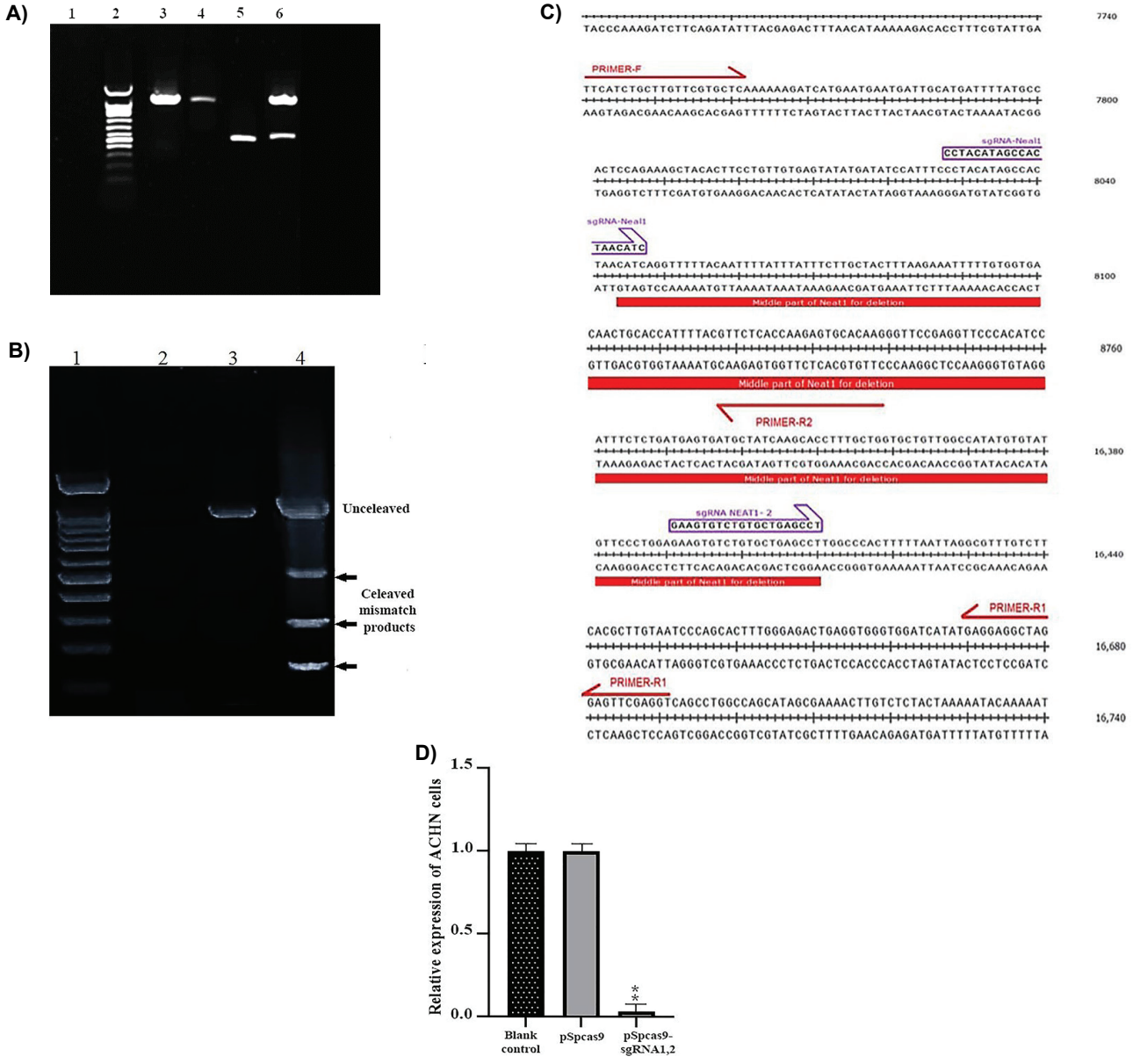

Figure 2. Gel electrophoresis of PCR fragments for *NEAT1* gene in ACHN cells. A) The presence of 590bp and 1001 bp fragments indicates *NEAT1-*/*NEAT1-*, *NEAT1+*/*NEAT1+* genotypes, respectively. Lane 1: Negative control PCR, lane 2: 100bp DNA Ladder, lane 3: non digest *NEAT1* gene with 1001 bp fragment in un-transfected cells (*NEAT1+* / *NEAT1+*), lane 4: non digest *NEAT1* gene with 1001 bp fragment in control group (*NEAT1+* /*NEAT1+*), lane 5: digested *NEAT1* gene with 590 bp fragment in pSpcas9-sgRNA1,2 group homozygous (*NEAT1-* / *NEAT1-*)**, l**ane 6: digested *NEAT1* gene with 590 bp and 1001 bp fragments in pSpcas9-sgRNA1,2 group heterozygous (*NEAT1-* / *NEAT1-*). **B)** The 1001bp and 590bp fragments were affected by T7 Endonuclease 1. 1) 100bp DNA Ladder 2) Negative control PCR 3**)** pSpcas9-group (control group) 4) Digested by T7E1. **C**) pSpcas9-sgRNA1,2 indicates deletion of the 8953 bp gene region generated using sgRNAs. **D)** *NEAT1* mRNA presence in 3 groups of ACHN cells was detected by RT-PCR. (** $p < 0.01$). *NEAT1: Nuclear paraspeckle assembly transcript 1, pSpcas9: pSpcas9 (BB) 2A- Puro V2.0 vector*

4.4. The NEAT1 Gene Knockout Lead to Increased Expression of Proapoptotic Genes

Both proapoptotic genes, *P53*, *BAK*, *FAS*, and *BAX* and antiapoptotic genes, *BCL2* and *SURVIVIN* were evaluated using quantitative real-time PCR (qRT-PCR) in the examined cell lines: the pSpcas9-sgRNA1, 2, pSpcas9-group, and blank control. Proapoptotic gene expression was significantly higher in the

pSpcas9-sgRNA1, 2 groups than pSpcas9 and blank control groups (**Fig. 3A**, p<0.01). We next assessed antiapoptotic gene (*BCL2*, *SURVIVIN*) expression in 3 different RCC ACHIN cell groups. *BCL2* and *SURVIVIN* gene expression was higher in the RCC control cell lines (pSpcas9-group, and blank control) than in crispr cas9 pSpcas9-sgRNA1, 2 cells ($p < 0.05$). The expressions of proapoptotic genes such as *P53*, *BAK*, *BAX*, and *FAS* increased in the ACHN cell line (pSpcas9-sgRNA1, 2 group) **(Fig. 3A**). The P-value for the proapoptotic *P53*, *BAK*, *BAX*, and *FAS* genes were 0.020, 0.016, 0.006, and 0.011, respectively, which indicates that these increases were statistically significant. In contrast, the expression of *BCL2* and *SURVIVIN* antiapoptotic genes showed a decrease in the ACHN cell line (pSpcas9-sgRNA1, 2 group). The P values for *BCL2* and anti-apoptotic SURVIVIN were 0.040 and 0.048, respectively (statistically significant).

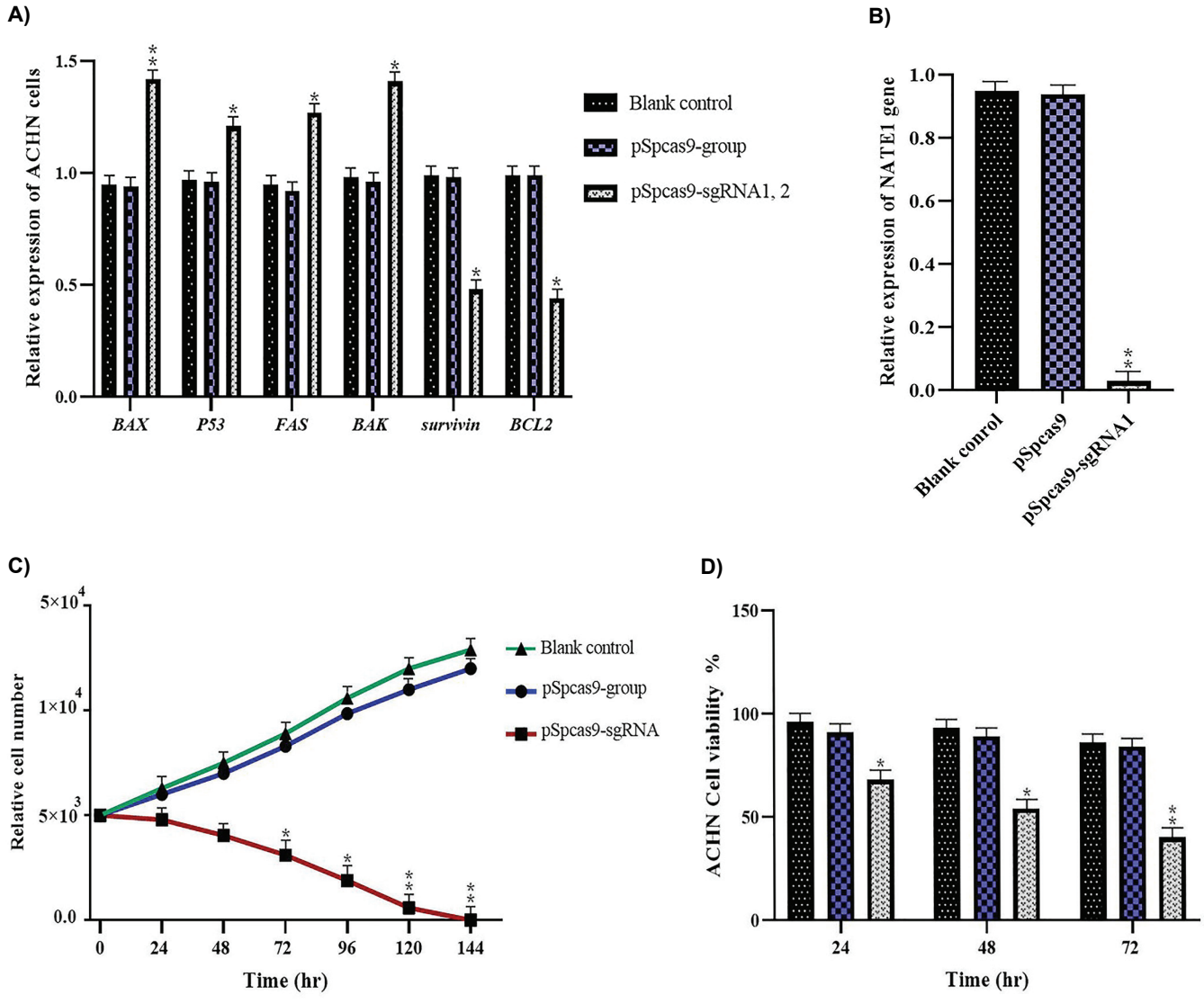

Figure 3. Knockout of *NEAT1* gene in ACHN cell line. A) induction of expression of pro-apoptotic genes *BAX, P53*, *FAS*, *BAK* at a significant level ** P <0.01 and reduction of expression of anti-apoptotic genes *SURVIVIN* and *BCL2* at a significant level * P <0.05. **B)** LncRNA *NEAT1* increases the proliferation of RCC cell lines. **C)** Different groups of ACHN cells expressing were cultured in 96-well plates, and cell proliferation was measured using CCK-8. **D)** Different groups of ACHN were cultured in 96- well plates and subjected to MTT assays to determine cell viability. *NEAT1: Nuclear paraspeckle assembly transcript 1, pSpcas9: pSpcas9 (BB) 2A- Puro V2.0 vector.*

As a result, knocking out the *NEAT1* gene enhances the production of apoptotic genes while decreasing the expression of antiapoptotic genes in the ACHN cancer cell line.

4.5. LncRNA NEAT1 Increases the Proliferation of Human RCC Cell Lines

NEAT1 silencing efficiency in RCC cell lines was assessed. We gathered ACHN human RCC cell lines (pSpcas9-sgRNA1,2, pSpcas9-group, and blank control) and used qRT–PCR to examine *NEAT1* expression in these cells. *NEAT1* was found to be the most highly expressed gene in both the pSpcas9 group and the blank control cell lines (**Fig. 3B**). These findings have shown that the *NEAT1* gene deletion in the pSpcas9-sgRNA1/2 group was carried out appropriately, with a considerable reduction in *NEAT1* expression ($P<0.01$). The CCK-8 assay was used to study the influence of *NEAT1* on the proliferation of RCC cell lines. Both the pSpcas9 group and the blank control ACHN cells had a high rate of cell proliferation. As a result, in the pSpcas9-sgRNA1/2 group, NEAT1 knockout decreased the proliferation of ACHN cells, as determined by the CCK-8 assay (**Fig. 3C**). Cell viability was evaluated using MTT assays 24 hours, 48 hours, and 72 hours after ACHN cells were grown in 96-well plates. Similarly, MTT experiments revealed that knocking out NEAT1 in the pSpcas9-sgRNA1/2 group reduced ACHN cell viability (**Fig. 3D**). Briefly, cell proliferation of ACHN cells was significantly inhibited by pSpcas9-sgRNA1/2 compared to the control groups ($p<0.01$). The results indicated that *NEAT1* knockout might inhibit ACHN RCC cell proliferation. Our results confirmed that lncRNA *NEAT1* promotes the proliferation of RCC cells.

4.6. lncRNA NEAT1 Promotes Cell Cycle Progression in RCC Cells

Cell cycle advancement is linked to the acceleration of cell proliferation. Flow cytometry was used to examine cell cycle regulation in the pSpcas9-sgRNA1/2, pSpcas9-group, and blank control group of ACHN cells (**Fig. 4A**). *NEAT1* knocked out ACHN cells with an increase in G0. G1 and a decrease in the S phase to G2.M phase ratio compared to the control groups (pSpcas9 group and blank control). *NEAT1* knockout hindered cell cycle progression, according to these findings.

4.7. knockout of LncRNA NEAT1 Promoted RCC Cells Apoptosis

The RCC cells, knocked out by pSpcas9-sgRNA1/2, experienced cell growth suppression and apoptosis. Flow cytometry was used to determine apoptosis in the pSpcas9-sgRNA1,2, pSpcas9-group, and blank control group of ACHN cells (**Fig. 4B**). In the pSpcas9-sgRNA1/2 group (**Fig. 4C**), the proportion of apoptotic cells was substantially higher than in the pSpcas9 group and the blank control group. *NEAT1* lncRNA decreased apoptosis in RCC cells, according to these findings.

4.8. NEAT1 Knockout Suppressed Cell Migration

Colony formation assays have shown that the number of clones in the pSpcas9-sgRNA1/2, pSpcas9-group and blank control of ACHN cells was reduced. The number of clones in the pSpcas9-sgRNA1/2 group was counted to show significant differences from the control groups (**Fig. 5B**). *NEAT1*'s effects on RCC cell migration were then studied. ACHN cell migration was inhibited by *NEAT1* knockout. The invasive potential of the pSpcas9-sgRNA1/2 group of ACHN cells was dramatically decreased in the Trans well cell invasion and metastasis experiment compared to the pSpcas9 group and blank control cells (**Fig. 5A**). At the same time, the number of cells invading the Trans well was counted, and the findings revealed that after knocking out *NEAT1*, the number of invasive RCC cells was dramatically reduced (**Fig. 5C**).

5. Discussion

RCC metastasis is one of the primary reasons for the failure of RCC therapy. On the other hand, traditional surgical therapy has been shown to be ineffective. For metastatic and progressing RCC, there is no powerful effectiveness. Radiation and chemotherapy do not affect it (27). Although targeted medications such as sorafenib and sunitinib have improved the longevity of patients with advanced RCC, there are still flaws, such as drug resistance (28). As a result, a novel RCC therapeutic target is a discovery. mRNA (such as HIF1-a, VEGF), miRNA (such as miR-21, miR-155), and lncRNA have all been identified as possible RCC molecular targets in recent years (29-32). LncRNAs offer a wide range of therapeutic applications in the diagnosis, treatment, and prognosis of malignancies, and they have become an investigation priority for cancers of the urinary system.

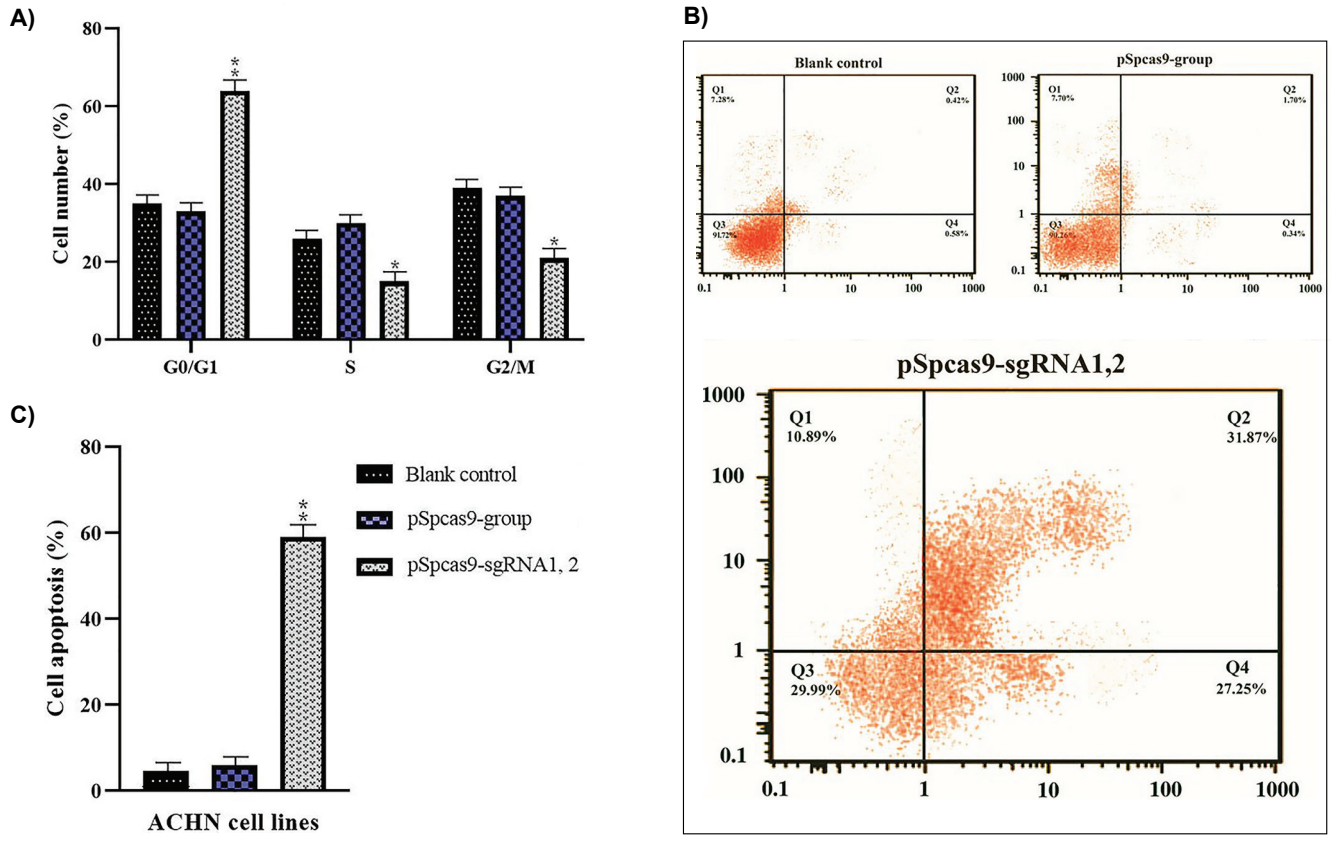

Figure 4. LncRNA *NEAT1* accelerates the cell cycle progression of RCC cells. A) Cell cycle assays were performed by flow cytometry. **B)** Knocking out the lncRNA *NEAT1* causes RCC cells to apoptosis. **C)** The fraction of apoptotic cells in the Q1, Q2, Q3, and Q4 quadrants of ACHN cells was calculated using Flowjo software. *P < 0.05; **P < 0.01. *NEAT1: Nuclear paraspeckle assembly transcript 1, pSpcas9: pSpcas9 (BB) 2A- Puro V2.0 vector.*

LncRNAs are RNA molecules that are longer than 200 nucleotides but do not encode proteins. LncRNAs are very diverse RNAs that play an essential role in the biological processes of various disorders, most notably cancers (33). In the biological control of cancers, such as the *P53* and NF-kB pathways, lncRNAs act as proto-oncogenes and tumor suppressor genes (34).

Although specific lncRNAs have been examined in RCC, such as MALAT1 and ATB, many more have yet to be found, and there is presently no lncRNA with RCC specificity (35-37). The lncRNA *NEAT1* was determined to be a newly identified RCC-associated lncRNA in our research. *NEAT1* was substantially expressed in RCC tissues and promoted RCC cell growth in vitro. As a result, we propose lncRNA *NEAT1* as a novel biomarker for the diagnosis and treatment of RCC. Several forms of lncRNAs have been discovered to have a role in tumor metastasis regulation. The lncRNA CCAT2 promoted tumor migration in HCC cells, but CCAT2 knockout inhibited invasion in highly metastatic HCC (38). The p53/Akt signaling pathway is controlled by lncRNA HOTAIR, which controls tumor metastasis in breast cancer cells (39).

Furthermore, HOTAIR was linked to metastasis, such as glioma, and a poor prognostic factor for glioma (40). According to our findings, the regulatory factor *NEAT1* for RCC tumor metastasis stimulates RCC cells. According to the RT- PCR, the lncRNA *NEAT1* were strongly expressed in the RCC control group compared to the pSpcas9-sgRNA1/2 group. *NEAT1* was shown to be substantially expressed in metastatic RCC tissues simultaneously. As a result, *NEAT1* could be used to predict RCC development and tumor spread. Cancer cells have high proliferative activity (41, 42).

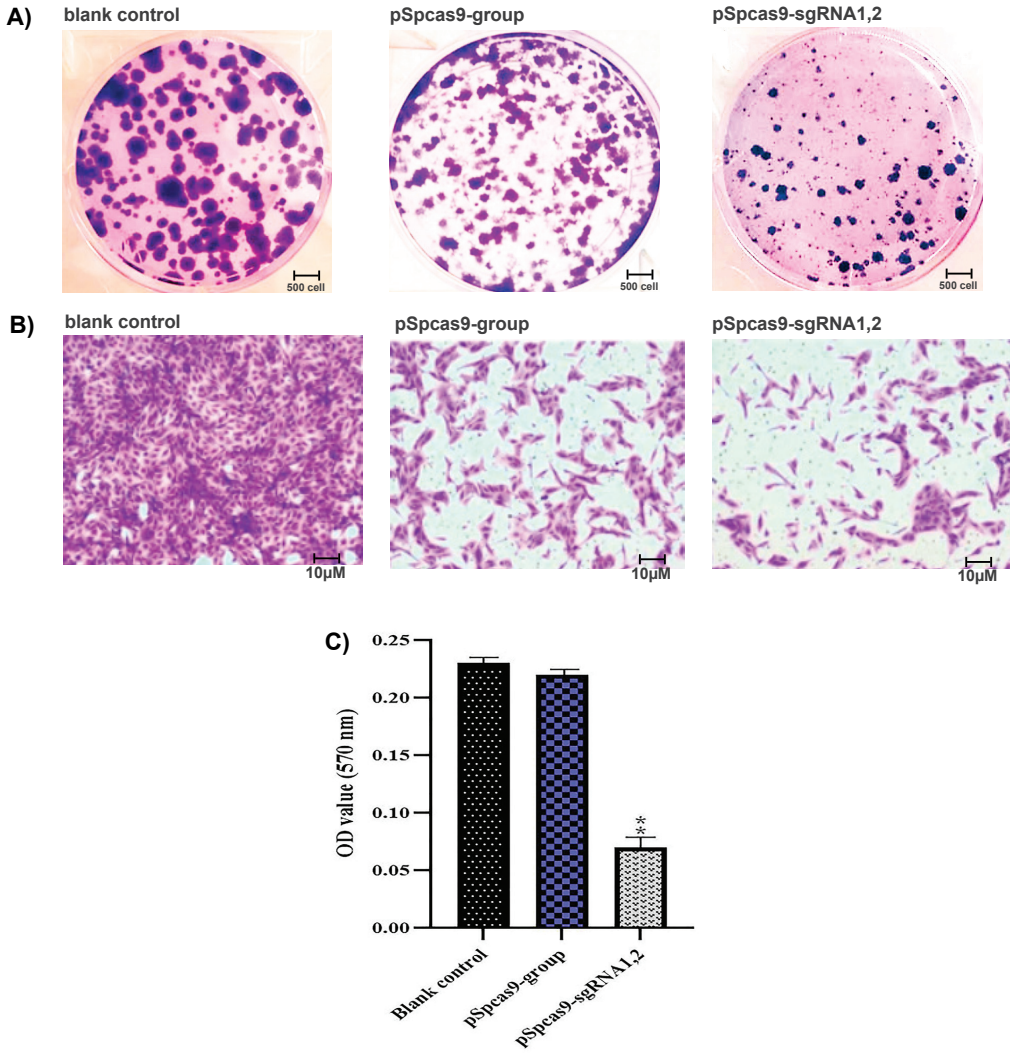

Figure 5. LncRNA *NEAT1* promotes the migration of RCC cells. A) Different group of ACHN cells were cultured in 6- well plates and subjected to colony formation assays. **B)** ACHN cells were seeded into transwells and invasive cells were imaged after 24 hours of culture. **C)** The quantitative analysis of the migrated ACHN cell groups. *NEAT1: Nuclear paraspeckle assembly transcript 1, pSpcas9: pSpcas9 (BB) 2A- Puro V2.0 vector*

NEAT1 has previously been linked to the progression of various malignancies (43, 44). Chen *et al*., found that overexpression of *NEAT1* increased the proliferation of esophageal squamous cell carcinoma (44). We discovered that blocking cell cycle progression by knocking out *NEAT1* inhibited RCC cell growth. These data, together with the high expression of NEAT1 in RCC tissue, imply that *NEAT1* may act as an oncogene promoting RCC's development (45, 46). In RCC patients, metastasis is the most common cause of death (47, 48). *NEAT1* knockout inhibits gastric cancer cell migration and invasion in vitro, according to previous research (49, 50). lncRNAs could provide a new landscape for research to determine the relationship between lncRNAs and metastasis cell and migration pathways (51, 52). Evidence supports the effect of lncRNA on drug resistance, increase or decrease in apoptosis, and cell proliferation (53, 54). Our findings showed that the out-regulation of *NEAT1* decreased RCC cells' capacity to migrate, which was in line with findings of other researchers (55, 56, 57). According to our findings, *NEAT1* knockout reduced antiapoptotic gene expression in RCC cells. *NEAT1* knockout also induced apoptosis in RCC cells by increasing proapoptotic genes. These findings show that *NEAT1*-targeted RCC treatments may be beneficial. Our findings are the

first to illustrate that knocking out *NEAT1* controlled RCC development by boosting proapoptotic genes (*P53*, *FAS*, *BAK*, and *BAX*).

6. Conclusion

To the best of our knowledge, this is the first investigation of the influence of *NEAT1* on kidney cancer cell progression. Furthermore, employing *NEAT1* as a target may have therapeutic benefits in generating possible therapies for kidney malignancies, demonstrating the need for a better knowledge of the biology of these diseases with direct clinical results for establishing innovative treatment options. Knockout of the *NEAT1* gene in the ACHN cell line using the CRISPR/Cas9 technique reduced cell survival and proliferation and increased apoptosis. Therefore, it seems that the inactivation of the *NEAT1* gene effectively increases the apoptosis of kidney cancer cells.

Acknowledgements

The authors would like to thank the staff members of the Biotechnology Research Center of Islamic Azad University of Shahrekord Branch in Iran for their help and support. This research did not receive any specific grant from funding agencies in the public, commercial, or not-for-profit sectors.

Conflict of Interest

The authors declare no conflict of interest

References

1. Capitanio U, Bensalah K, Bex A, Boor Jian S, Bray F, Coleman J, *et al*. Epidemiology of Renal Cell Carcinoma. *Eur Urol*. 2019;**75**(1):74-84. doi:10.1016/j.eururo.2018.08.036
2. Hardiman O, Al-Chalabi A, Chio A, Corr EM, Logroscino G, Robberecht W, Shaw PJ, Simmons Z, Van Den Berg LH. Amyotrophic lateral sclerosis. *Nat Rev Dis Primers*. 2017;**3**(1):1-9. doi: 10.1038/nrdp.2017.71
3. Motzer RJ, Jonasch E, Michaelson MD, Nandagopal L, Gore JL, George S, *et al*. Featured updates to the NCCN guidelines. *JNCCN*. 2019;**17**(11):1278-1285. doi:10.6004/jnccn.2019.0054
4. Low G, Huang G, Fu W, Moloo Z, Girgis S. Review of renal cell carcinoma and its common subtypes in radiology. *World J Radiol*. 2016;**8**(5):484. doi:10.4329/wjr.v8.i5.484
5. Garje R, A J, Greco A, Vaddepally RK, Zakharia Y. The future of immunotherapy-based combination therapy in metastatic renal cell carcinoma. *Cancers*. 2020;**12**(1):143. doi:10.3390/cancers12010143
6. Safiri S, Kolahi AA, Mansournia MA, Almasi-Hashiani A, Ashrafi-Asgarabad A, Sullman MJ, Bettampadi D, Qorbani M, Moradi-Lakeh M, Ardalan M, Mokdad A. The burden of kidney cancer and its attributable risk factors in 195 countries and territories, 1990–2017. *Sci Rep*. 2020;**10**(1):1-20. doi:10.1038/s41598-020-70840-2
7. Statello L, Guo CJ, Chen LL, Huarte M. Gene regulation by long noncoding RNAs and its biological functions. *Nat Rev Mol Cell Biol*. 2021;**22**(2):96-118. doi:10.1038/s41580-020-00315-9
8. Karakas D, Ozpolat B. The role of LncRNAs in translation. *Non-coding RNA*. 2021;**7**(1):16. doi:10.3390/ncrna7010016
9. Li JK, Chen C, Liu JY, Shi JZ, Liu SP, Liu B, Wu DS, Fang ZY, Bao Y, Jiang MM, Yuan JH. Long noncoding RNA MRCCAT1 promotes metastasis of clear cell renal cell carcinoma by inhibiting NPR3 and activating p38-MAPK signaling. *Mol Cancer*. 2017;**16**(1):1-4. doi:10.1186/s12943-017-0681-0.
10. Li Y, *et al*. Identification of long-non coding RNA UCA1 as an oncogene inrenal cell carcinoma. *Mol Med Rep*. 2016;**13**(4):3326-3334. doi:10.3892/mmr.2016.4894
11. Xiong J, *et al*. High expression of long noncoding RNA lncRNA-ATB iscorrelated with metastases and promotes cell migration and invasion inrenal cell carcinoma. *Jpn J Clin Oncol*. 2016;**46**(4):378-384. doi:10.1093/jjco/hyv214
12. Wang L, *et al*. Out-regulated long noncoding RNA H19 inhibitscarcinogenesis of renal cell carcinoma. *Neoplasma*. 2015;**62**(3):412-418. doi:10.4149/neo_2015_049
13. He X, *et al*. Knockout of Long noncoding RNA FTX inhibits proliferation, migration, and invasion in renal cell carcinoma cells. *Oncol Res*. 2017;**25**(2):157-166. doi:10.3727/096504016X14719078133203
14. Dong P, Xiong Y, Yue J, Hanley SJ, Kobayashi N, Todo Y, Watari H. Long noncoding RNA NEAT1: a novel target for diagnosis and therapy in human tumors. *Front. Genet*.2018;**9**:471. doi:10.3389/fgene.2018.00471
15. Standaert L, Adriaens C, Radaelli E, Van Keymeulen A, Blanpain C, Hirose T, Nakagawa S, Marine JC. The long noncoding RNA Neat1 is required for mammary gland development and lactation. *Rna*. 2014;**20**(12):1844-1849. doi:10.1261/rna.047332.114
16. Lanzos Camaioni AA, Carlevaro-Fita J, Mularoni L, Reverter F, Palumbo E, Guigó Serra R, Johnson R. Discovery of Cancer Driver Long Noncoding RNAs across 1112 Tumor Genomes: New Candidates and Distinguishing Features. *Sci Rep*. 2017;**7**:41544. doi:10.1038/srep41544
17. Parasramka MA, Maji S, Matsuda A, Yan IK, Patel T. Long noncoding RNAs as novel targets for therapy in hepatocellular carcinoma. *Pharmacol Ther*.2016;**161**:67-78. doi:10.1016/j.pharmthera.2016.03.004
18. Worku T, Bhattarai D, Ayers D, Wang K, Wang C, ur Rehman Z, sajjad Talpur H, Yang L. Long noncoding RNAs: the new horizon of gene regulation in ovarian cancer. *Cell Physiol Biochem*. 2017;**44**(3):948-966. doi:10.1159/000485395
19. Arun G, Diermeier SD, Spector DL. Therapeutic targeting of long noncoding RNAs in cancer. *Trends Mol Med.* 2018;**24**(3):257-277. doi:10.1016/j.molmed.2018.01.001
20. Uddin F, Rudin CM, Sen T. CRISPR gene therapy: applications, limitations, and implications for the future. *Front Oncol.* 2020;**10**:1387. doi:10.3389/fonc.2020.01387
21. Loureiro A, da Silva GJ. Crispr-cas: Converting a bacterial defense mechanism into a state-of-the-art genetic manipulation tool. *Antibiotics*. 2019;**8**(1):18. doi:10.3390/antibiotics8010018

22. Zhang Y, Showalter AM. CRISPR/Cas9 genome editing technology: a valuable tool for understanding plant cell wall biosynthesis and function. *Front Plant Sci*. 2020;**11**. doi:10.3389/fpls.2020.589517
23. Liu X, Hao Y, Yu W, Yang X, Luo X, Zhao J, Li J, Hu X, Li L. Long noncoding RNA emergence during renal cell carcinoma tumorigenesis. *Cell Physiol Biochem*. 2018;**47**(2):735-746. doi:10.1159/000490026
24. Creager AN. Recipes for recombining DNA: A history of Molecular Cloning: A Laboratory Manual. *BJHS Themes*. 2020;**5**:225-243. doi:10.1017/bjt.2020.5
25. Narimani M, Sharifi M, Jalili A. Knockout of BIRC5 gene by CRISPR/Cas9 induces apoptosis and inhibits cell proliferation in leukemic cell lines, HL60 and KG1. *Biol Targets Ther*. 2019;**9**:53. doi:10.2147/BLCTT.S230383
26. Zhen S, Hua L, Liu YH, Sun XM, Jiang MM, Chen W, Zhao L, Li X. Inhibition of long noncoding RNA UCA1 by CRISPR/Cas9 attenuated malignant phenotypes of bladder cancer. Oncotarget. 2017;**8**(6):9634. doi:10.18632/oncotarget.14176
27. Emmanuel M, David P, Guillemette B, *et al*. Stereotactic radiation therapy in the strategy of treatment of metastatic renal cell carcinoma: a study of the Getug group. *Eur J Cancer*. 2018;**98**:38-47. doi:10.1016/j.ejca.2018.04.008
28. Buchler T, Klapka R, Melichar B, *et al*. Sunitinib followed by sorafenib or vice versa for metastatic renal cell carcinoma—data from the Czech registry. *Ann Oncol*. 2012;**23**(2):395-401. doi:10.1093/annonc/mdr065
29. Okabe T, Kumagai M, Ikeda M, *et al*. The impact of HIF1A/ARNT on the PER2 transcriptional activity in renal cancer cells. *J Urology*. 2013;**189**(4): e122. doi:10.1016/j.juro.2013.02.1685
30. Powles T, Staehler M, Ljungberg B, *et al*. Updated EAU guidelines for clear cell renal cancer patients who fail VEGF targeted therapy. *Eur Urol*. 2016;**69**(1):4-6. doi:10.1016/j.eururo.2015.10.0170302-2838/#2015
31. Wang G, Kwan CH, Lai MM, *et al*. Elevated levels of miR-146a and miR-155 in kidney biopsy and urine from patients with IgA nephropathy. *Dis Markers*. 2011;**30**(4):171-179. doi:10.3233/DMA-2011-0766
32. Chen J, Gu Y, Shen W. MicroRNA-21 functions as an oncogene and promotes cell proliferation and invasion via TIMP3 in renal cancer. *Eur Rev Med Pharmacol Sci*. 2017;**21**(20):4566-4576.
33. Silva A, Bullock M, Calin G. The clinical relevance of long noncoding RNAs in cancer. *Cancers*. 2015;**7**(4):2169-2182. doi:10.3390/cancers7040884
34. Eswar S, Ailin Z, Daniel F, Gupta S. Betulinic acid-mediated apoptosis in human prostate cancer cells involves *P53* and nuclear factor-kappa B (NF-kB) Pathways. *Molecules*. 2017;**22**(2):264. doi:10.3390/molecules22020264
35. Xiao H, Tang K, Liu P, *et al*. LncRNA MALAT1 functions as a competing endogenous RNA to regulate ZEB2 expression by sponging miR-200 s in clear cell kidney carcinoma. *Oncotarget*. 2015;**6**(35):38005-38015. doi:10.18632/oncotarget.5357
36. Qi JJ, Liu YX, Lin L. High expression of long noncoding RNA ATB is associated with poor prognosis in patients with renal cell carcinoma. *Eur Rev Med Pharmacol Sci*. 2017;**21**(12):2835-2839.
37. Ning L, Li Z, Wei D, *et al*. LncRNA, *NEAT1* is a prognosis biomarker and regulates cancer progression via epithelial mesenchymal transition in clear cell renal cell carcinoma. *Cancer Biomark*. 2017;**19**(1):75-83. doi:10.3233/CBM-160376
38. Zhou N, Si Z, Li T, *et al*. Long noncoding RNA CCAT2 functions as an oncogene in hepatocellular carcinoma, regulating cellular proliferation, migration and apoptosis. *Oncology Lett*. 2016;**12**(1):132-138. doi:10.3892/ol.2016.4580
39. Yu Y, Lv F, Liang D, *et al*. HOTAIR may regulate proliferation, apoptosis, migration and invasion of MCF-7 cells through regulating the *P53*/Akt/JNK signaling pathway. *Biomed Pharmacot*. 2017;**90**:555-561. doi:10.1016/j.biopha.2017.03.054
40. Zhou X, Ren Y, Zhang J, *et al*. HOTAIR is a therapeutic target in glioblastoma. *Oncotarget*. 2015;**6**(10):8353-8365. doi:10.18632/oncotarget.3229
41. Wangsa D, Ryott M, Avall-Lundqvist E, Petersson F, Elmberger G, Luo J, Ried T, Auer G, Munck-Wikland E. Ki-67 expression predicts locoregional recurrence in stage I oral tongue carcinoma. *Br J Cancer*. 2008;**99**:1121-1128. doi: 10.1038/sj.bjc.6604633
42. Kuper C, Beck FX, Neuhofer W. Autocrine MCP-1/CCR2 signaling stimulates proliferation and migration of renal carcinoma cells. *Oncol Lett*. 2016;**12**:2201-2209. doi:10.3892/ol.2016.4875
43. Jiang P, Wu X, Wang X, Huang W, Feng Q. *NEAT1* upregulates EGCG-induced CTR1 to enhance cisplatin sensitivity in lung cancer cells. *Oncotarget*. 2016;**7**:43337-43351. doi:10.18632/oncotarget.9712.
44. Chen X, Kong J, Ma Z, Gao S, Feng X. Up regulation of the long noncoding RNA *NEAT1*promotes esophageal squamous cell carcinoma cell progression and correlates with poor prognosis. *Am J Cancer Res*. 2015;**5**:2808-2815.
45. Torregrossa L, Rotondo MI, Insilla AC, Galleri D, Guidoccio F, Miccoli P, Livolsi VA, Basolo F. Metastasis of renal cell carcinoma to the parathyroid gland 16 years after radical nephrectomy: a case report. *Oncol Lett*. 2016;**12**:3224-3228. doi:10.3892/ol.2016.5071
46. Fu JW, Kong Y, Sun X. Long noncoding RNA *NEAT1* is an unfavorable prognostic factor and regulates migration and invasion in gastric cancer. *J Cancer Res Clin Oncol*. 2016;**142**:1571-1579. doi:10.1007/s00432-016-2152-1
47. Piri Gharaghie T, Beiranvand S, Doosti A, Ghadiri AH, Haji Mohammadi S. A review of the epidemiology and clinical signs of SARS-COV-2. *NCMB J* 2020,**11**(41): 103-120.
48. Karimi M, Ghazikhanlou-Sani K, Mehdizadeh AR, Mostaghimi H. Lead-free transparent shields for diagnostic X-rays: Monte Carlo simulation and measurements. *Radiol. Phys. Technol*. 2020;**13**(3):276-87.
49. Abdian N, Ghasemi-Dehkordi P, Hashemzadeh-Chaleshtori M, Ganji-Arjenaki M, Doosti A, Amiri B. Comparison of human dermal fibroblasts (HDFs) growth rate in culture media supplemented with or without basic fibroblast growth factor (bFGF). *Cell Tissue Bank*. 2015;**16**(4):487-495. doi:10.1007/s10561-015-9494-9
50. Zarinnezhad, Amineh, Shah Hosseini, Mohammad Hassan, Piri Gharaghie T. Evaluation of relative frequency of fungal infections in serum of patients with multiple sclerosis and healthy individuals by PCR. *BJM*. 2021;**10**(37):37-50. doi: 10.22108/bjm.2020.122265.1288
51. Mostaghimi H, Ahmadabad FG, Rezaei H. Super-selective intra-arterial platinum-based chemotherapy concurrent with

low-dose-rate plaque brachytherapy in the treatment of retinoblastoma: A simulation study. *J Cancer Res Ther.* 2021; **17**(1):130.

52. Ansari H, Tahmasebi-Birgani M, Bijanzadeh M, Doosti A, Kargar M. Study of the immunogenicity of outer membrane protein A (ompA) gene from Acinetobacter baumannii as DNA vaccine candidate *in vivo*. *Iran J Basic Med Sci*. 2019;**22**(6):669-675.
53. Gharaghie TP, Beiranvand S, Riahi A, Badmasti F, Shirin NJ, Mirzaie A, Elahianfar Y, Ghahari S, Ghahari S, Pasban K, Hajrasoliha S. Fabrication and characterization of thymol-loaded chitosan nanogels: improved antibacterial and anti-biofilm activities with negligible cytotoxicity. *Chemistry & biodiversity*. 2022. doi:10.1002/cbdv.202100426
54. Gharaghie TP, Beiranvand S, Hajimohammadi S. Comparison of Antifungal Effects of Aquatic and Alcoholic Extract of Mentha pulegium L.With Fluconazole on Growth of Candida Albicans. *JDB*. 2021;**13**(2):718.
55. Safarpour-Dehkordi M, Doosti A, Jami MS. Impacts of the Staphylococcal Enterotoxin H on the Apoptosis and lncRNAs in PC3 and ACHN. *Mol Genet Microbiol Virol*. 2020;**35**(3):180-188. doi:10.3103/S0891416820030076
56. Safarpour-Dehkordi M, Doosti A, Jami MS. Integrative analysis of lncRNAs in kidney cancer to discover a new lncRNA (LINC00847) as a therapeutic target for staphylococcal enterotoxin tst gene. *Cell J. (Yakhteh)*. 2020;**22**(Suppl 1):101. doi:10.22074/cellj.2020.6996
57. Piri-Gharaghie T, Jegargoshe-Shirin N, Saremi-Nouri S, Khademhosseini SH, Hoseinnezhad-Lazarjani E, Mousavi A, Kabiri H, Rajaei N, Riahi A, Farhadi-Biregani A, Fatehi-Ghahfarokhi S. Effects of Imipenem-containing Niosome nanoparticles against high prevalence methicillin-resistant Staphylococcus Epidermidis biofilm formed. *Scientific Reports*. 2022;**12**(1):1-3. doi:10.1038/s41598-022-09195-9.